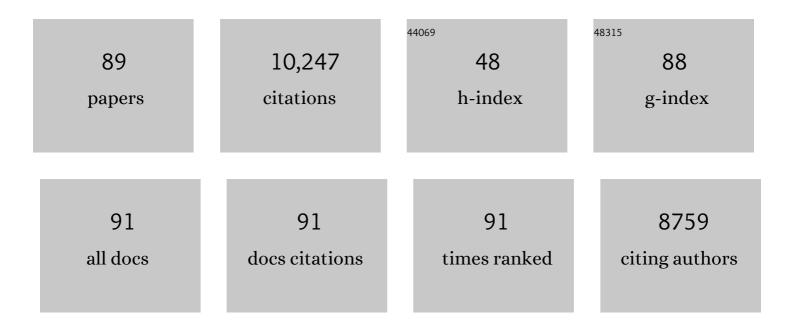
List of Publications by Year in descending order

Source: https://exaly.com/author-pdf/336098/publications.pdf Version: 2024-02-01



FENC HE

#	Article	IF	CITATIONS
1	Surface functional groups of carbon-based adsorbents and their roles in the removal of heavy metals from aqueous solutions: A critical review. Chemical Engineering Journal, 2019, 366, 608-621.	12.7	790
2	Preparation and Characterization of a New Class of Starch-Stabilized Bimetallic Nanoparticles for Degradation of Chlorinated Hydrocarbons in Water. Environmental Science & Technology, 2005, 39, 3314-3320.	10.0	736
3	Stabilization of Feâ^Pd Nanoparticles with Sodium Carboxymethyl Cellulose for Enhanced Transport and Dechlorination of Trichloroethylene in Soil and Groundwater. Industrial & Engineering Chemistry Research, 2007, 46, 29-34.	3.7	586
4	Manipulating the Size and Dispersibility of Zerovalent Iron Nanoparticles by Use of Carboxymethyl Cellulose Stabilizers. Environmental Science & Technology, 2007, 41, 6216-6221.	10.0	510
5	Biochar technology in wastewater treatment: A critical review. Chemosphere, 2020, 252, 126539.	8.2	482
6	Field assessment of carboxymethyl cellulose stabilized iron nanoparticles for in situ destruction of chlorinated solvents in source zones. Water Research, 2010, 44, 2360-2370.	11.3	368
7	Effects of ball milling on the physicochemical and sorptive properties of biochar: Experimental observations and governing mechanisms. Environmental Pollution, 2018, 233, 54-63.	7.5	314
8	Adsorptive removal of arsenate from aqueous solutions by biochar supported zero-valent iron nanocomposite: Batch and continuous flow tests. Journal of Hazardous Materials, 2017, 322, 172-181.	12.4	263
9	Mechanochemically Sulfidated Microscale Zero Valent Iron: Pathways, Kinetics, Mechanism, and Efficiency of Trichloroethylene Dechlorination. Environmental Science & Technology, 2017, 51, 12653-12662.	10.0	262
10	Experimental and modeling investigations of ball-milled biochar for the removal of aqueous methylene blue. Chemical Engineering Journal, 2018, 335, 110-119.	12.7	262
11	Environmental occurrences, fate, and impacts of microplastics. Ecotoxicology and Environmental Safety, 2019, 184, 109612.	6.0	259
12	Transport of carboxymethyl cellulose stabilized iron nanoparticles in porous media: Column experiments and modeling. Journal of Colloid and Interface Science, 2009, 334, 96-102.	9.4	245
13	Dechlorination of Excess Trichloroethene by Bimetallic and Sulfidated Nanoscale Zero-Valent Iron. Environmental Science & Technology, 2018, 52, 8627-8637.	10.0	240
14	Composition and functional group characterization of extracellular polymeric substances (EPS) in activated sludge: the impacts of polymerization degree of proteinaceous substrates. Water Research, 2018, 129, 133-142.	11.3	232
15	Hydrodechlorination of trichloroethene using stabilized Fe-Pd nanoparticles: Reaction mechanism and effects of stabilizers, catalysts and reaction conditions. Applied Catalysis B: Environmental, 2008, 84, 533-540.	20.2	215
16	Atomically Defined Undercoordinated Active Sites for Highly Efficient CO ₂ Electroreduction. Advanced Functional Materials, 2020, 30, 1907658.	14.9	210
17	Ball-Milled Carbon Nanomaterials for Energy and Environmental Applications. ACS Sustainable Chemistry and Engineering, 2017, 5, 9568-9585.	6.7	187
18	Degradation of soil-sorbed trichloroethylene by stabilized zero valent iron nanoparticles: Effects of sorption, surfactants, and natural organic matter. Water Research, 2011, 45, 2401-2414.	11.3	180

#	Article	IF	CITATIONS
19	Enhanced adsorption performance and governing mechanisms of ball-milled biochar for the removal of volatile organic compounds (VOCs). Chemical Engineering Journal, 2020, 385, 123842.	12.7	176
20	Immobilization of mercury in sediment using stabilized iron sulfide nanoparticles. Water Research, 2009, 43, 5171-5179.	11.3	163
21	Enhanced lead and cadmium removal using biochar-supported hydrated manganese oxide (HMO) nanoparticles: Behavior and mechanism. Science of the Total Environment, 2018, 616-617, 1298-1306.	8.0	163
22	Rapid and highly selective removal of lead from water using graphene oxide-hydrated manganese oxide nanocomposites. Journal of Hazardous Materials, 2016, 314, 32-40.	12.4	155
23	Reclaiming phosphorus from secondary treated municipal wastewater with engineered biochar. Chemical Engineering Journal, 2019, 362, 460-468.	12.7	136
24	Ball milling biochar iron oxide composites for the removal of chromium (Cr(VI)) from water: Performance and mechanisms. Journal of Hazardous Materials, 2021, 413, 125252.	12.4	135
25	Solvent-free synthesis of magnetic biochar and activated carbon through ball-mill extrusion with Fe3O4 nanoparticles for enhancing adsorption of methylene blue. Science of the Total Environment, 2020, 722, 137972.	8.0	131
26	In situ testing of metallic iron nanoparticle mobility and reactivity in a shallow granular aquifer. Journal of Contaminant Hydrology, 2010, 116, 35-46.	3.3	125
27	Insight into the kinetics and mechanism of removal of aqueous chlorinated nitroaromatic antibiotic chloramphenicol by nanoscale zero-valent iron. Chemical Engineering Journal, 2018, 334, 508-518.	12.7	123
28	Recent Advances in Sulfidated Zerovalent Iron for Contaminant Transformation. Environmental Science & Technology, 2021, 55, 8464-8483.	10.0	123
29	Role of dissolved Mn(III) in transformation of organic contaminants: Non-oxidative versus oxidative mechanisms. Water Research, 2017, 111, 234-243.	11.3	115
30	Chromium(VI) removal by mechanochemically sulfidated zero valent iron and its effect on dechlorination of trichloroethene as a co-contaminant. Science of the Total Environment, 2019, 650, 419-426.	8.0	108
31	In situ remediation technologies for mercury-contaminated soil. Environmental Science and Pollution Research, 2015, 22, 8124-8147.	5.3	102
32	Sulfidation mitigates the passivation of zero valent iron at alkaline pHs: Experimental evidences and mechanism. Water Research, 2019, 159, 233-241.	11.3	97
33	Rapid Removal of Hg(II) from Aqueous Solutions Using Thiol-Functionalized Zn-Doped Biomagnetite Particles. ACS Applied Materials & Interfaces, 2012, 4, 4373-4379.	8.0	96
34	Highly Boosted Reaction Kinetics in Carbon Dioxide Electroreduction by Surfaceâ€Introduced Electronegative Dopants. Advanced Functional Materials, 2021, 31, 2008146.	14.9	88
35	Degradation of Trichloroethene with a Novel Ball Milled Fe–C Nanocomposite. Journal of Hazardous Materials, 2015, 300, 443-450.	12.4	87
36	Polysugar-Stabilized Pd Nanoparticles Exhibiting High Catalytic Activities for Hydrodechlorination of Environmentally Deleterious Trichloroethylene. Langmuir, 2008, 24, 328-336.	3.5	85

#	Article	IF	CITATIONS
37	Highly active metallic nickel sites confined in N-doped carbon nanotubes toward significantly enhanced activity of CO2 electroreduction. Carbon, 2019, 150, 52-59.	10.3	84
38	Carboxymethyl cellulose stabilized and sulfidated nanoscale zero-valent iron: Characterization and trichloroethene dechlorination. Applied Catalysis B: Environmental, 2020, 262, 118303.	20.2	81
39	Precise Seed-Mediated Growth and Size-Controlled Synthesis of Palladium Nanoparticles Using a Green Chemistry Approach. Langmuir, 2009, 25, 7116-7128.	3.5	80
40	Manganese oxide nanoparticles impregnated graphene oxide aggregates for cadmium and copper remediation. Chemical Engineering Journal, 2018, 350, 1135-1143.	12.7	77
41	Sulfidation of Zero-Valent Iron by Direct Reaction with Elemental Sulfur in Water: Efficiencies, Mechanism, and Dechlorination of Trichloroethylene. Environmental Science & Technology, 2021, 55, 645-654.	10.0	69
42	A Universal Principle to Accurately Synthesize Atomically Dispersed Metal–N4 Sites for CO2 Electroreduction. Nano-Micro Letters, 2020, 12, 108.	27.0	65
43	One-Step "Green―Synthesis of Pd Nanoparticles of Controlled Size and Their Catalytic Activity for Trichloroethene Hydrodechlorination. Industrial & Engineering Chemistry Research, 2009, 48, 6550-6557.	3.7	64
44	Transport of stabilized iron nanoparticles in porous media: Effects of surface and solution chemistry and role of adsorption. Journal of Hazardous Materials, 2017, 322, 284-291.	12.4	63
45	Time-Dependent Density Functional Theory Assessment of UV Absorption of Benzoic Acid Derivatives. Journal of Physical Chemistry A, 2012, 116, 11870-11879.	2.5	55
46	Accelerated antimony and copper removal by manganese oxide embedded in biochar with enlarged pore structure. Chemical Engineering Journal, 2020, 402, 126021.	12.7	55
47	Coincorporation of N and S into Zero-Valent Iron to Enhance TCE Dechlorination: Kinetics, Electron Efficiency, and Dechlorination Capacity. Environmental Science & Technology, 2021, 55, 16088-16098.	10.0	53
48	Bi/Bi2O3 nanoparticles supported on N-doped reduced graphene oxide for highly efficient CO2 electroreduction to formate. Chinese Chemical Letters, 2020, 31, 1415-1421.	9.0	51
49	Quantifying the efficiency and selectivity of organohalide dechlorination by zerovalent iron. Environmental Sciences: Processes and Impacts, 2020, 22, 528-542.	3.5	51
50	Degradation kinetics and mechanisms of phenol in photo-Fenton process. Journal of Zhejiang University Science B, 2004, 5, 198-205.	0.4	51
51	FeN <i>_X</i> (C)-Coated Microscale Zero-Valent Iron for Fast and Stable Trichloroethylene Dechlorination in both Acidic and Basic pH Conditions. Environmental Science & Technology, 2021, 55, 5393-5402.	10.0	49
52	Photochemical Oxidation of Dissolved Elemental Mercury by Carbonate Radicals in Water. Environmental Science and Technology Letters, 2014, 1, 499-503.	8.7	48
53	Enhanced Fluoride Removal from Water by Nanoporous Biochar-Supported Magnesium Oxide. Industrial & Engineering Chemistry Research, 2019, 58, 9988-9996.	3.7	46
54	Arsenic (III) removal by mechanochemically sulfidated microscale zero valent iron under anoxic and oxic conditions. Water Research, 2021, 198, 117132.	11.3	45

#	Article	IF	CITATIONS
55	Oxygen-Content-Controllable Graphene Oxide from Electron-Beam-Irradiated Graphite: Synthesis, Characterization, and Removal of Aqueous Lead [Pb(II)]. ACS Applied Materials & Interfaces, 2016, 8, 25289-25296.	8.0	44
56	Adsorption of acetone and cyclohexane onto CO2 activated hydrochars. Chemosphere, 2020, 245, 125664.	8.2	43
57	Ultrafast sequestration of cadmium and lead from water by manganese oxide supported on a macro-mesoporous biochar. Chemical Engineering Journal, 2020, 387, 124095.	12.7	38
58	Mechanistic role of nitrate anion in TCE dechlorination by ball milled ZVI and sulfidated ZVI: Experimental investigation and theoretical analysis. Journal of Hazardous Materials, 2021, 403, 123844.	12.4	38
59	Mercury photolytic transformation affected by low-molecular-weight natural organics in water. Science of the Total Environment, 2012, 416, 429-435.	8.0	30
60	Ball-milled biochar for alternative carbon electrode. Environmental Science and Pollution Research, 2019, 26, 14693-14702.	5.3	30
61	Sulfidation enhances stability and mobility of carboxymethyl cellulose stabilized nanoscale zero-valent iron in saturated porous media. Science of the Total Environment, 2020, 718, 137427.	8.0	30
62	Insight into the fenton-induced degradation process of extracellular polymeric substances (EPS) extracted from activated sludge. Chemosphere, 2019, 234, 318-327.	8.2	28
63	Metal Foam-Based Fenton-Like Process by Aeration. ACS Omega, 2017, 2, 6104-6111.	3.5	26
64	Tea waste-supported hydrated manganese dioxide (HMO) for enhanced removal of typical toxic metal ions from water. RSC Advances, 2015, 5, 88900-88907.	3.6	25
65	Effects of non-reducible dissolved solutes on reductive dechlorination of trichloroethylene by ball milled zero valent irons. Journal of Hazardous Materials, 2020, 396, 122620.	12.4	25
66	Highly Efficient Sulfonic/Carboxylic Dualâ€Acid Synergistic Catalysis for Esterification Enabled by Sulfurâ€Rich Graphene Oxide. ChemSusChem, 2017, 10, 3352-3357.	6.8	21
67	Foamed urea-formaldehyde microspheres for removal of heavy metals from aqueous solutions. Chemosphere, 2020, 241, 125004.	8.2	21
68	Phosphate removal by lead-exhausted bioadsorbents simultaneously achieving lead stabilization. Chemosphere, 2017, 168, 748-755.	8.2	20
69	Nanocarbon-based catalysts for esterification: Effect of carbon dimensionality and synergistic effect of the surface functional groups. Carbon, 2019, 147, 134-145.	10.3	19
70	Stability of hydrous ferric oxide nanoparticles encapsulated inside porous matrices: Effect of solution and matrix phase. Chemical Engineering Journal, 2018, 347, 870-876.	12.7	18
71	Formation of Soluble Mercury Oxide Coatings: Transformation of Elemental Mercury in Soils. Environmental Science & Technology, 2015, 49, 12105-12111.	10.0	17
72	Esterification of fatty acids from waste cooking oil to biodiesel over a sulfonated resin/PVA composite. Catalysis Science and Technology, 2016, 6, 5590-5598.	4.1	15

#	Article	IF	CITATIONS
73	Highly selective and ultrafast removal of cadmium and copper from water by magnetic core-shell microsphere. Chemical Engineering Journal, 2021, 405, 126576.	12.7	13
74	Mechanochemically Sulfidated Zero Valent Iron as an Efficient Fenton-like Catalyst for Degradation of Organic Contaminants. Acta Chimica Sinica, 2017, 75, 866.	1.4	13
75	Transformation of the phyllomanganate vernadite to tectomanganates with small tunnel sizes: Favorable geochemical conditions and fate of associated Co. Geochimica Et Cosmochimica Acta, 2021, 295, 224-236.	3.9	12
76	Preparation and characterization of activated aluminum powder by magnetic grinding method for hydrogen generation. International Journal of Energy Research, 2014, 38, 1016-1023.	4.5	10
77	Enhanced dechlorination of trichloroethene by sulfidated microscale zero-valent iron under low-frequency AC electromagnetic field. Journal of Hazardous Materials, 2022, 423, 127020.	12.4	10
78	Impact of dissolved O ₂ on phenol oxidation by δ-MnO ₂ . Environmental Sciences: Processes and Impacts, 2019, 21, 2118-2127.	3.5	9
79	Characterization of aerobic granules formed in an aspartic acid fed sequencing batch reactor under unfavorable hydrodynamic selection conditions. Chemosphere, 2020, 260, 127600.	8.2	9
80	Sorption of Non-ionic Aromatic Organics to Mineral Micropores: Interactive Effect of Cation Hydration and Mineral Charge Density. Environmental Science & Technology, 2019, 53, 3067-3077.	10.0	8
81	Response to Comment on "Manipulating the Size and Dispersibility of Zerovalent Iron Nanoparticles by Use of Carboxymethyl Cellulose Stabilizers― Environmental Science & Technology, 2008, 42, 3480-3480.	10.0	6
82	Catalytic activity of noble metal nanoparticles toward hydrodechlorination: influence of catalyst electronic structure and nature of adsorption. Frontiers of Environmental Science and Engineering, 2015, 9, 888-896.	6.0	6
83	Deciphering CaO-induced peroxydisulfate activation for destruction of halogenated organic pollutants in a low energy vibrational mill. Chemical Engineering Journal, 2022, 431, 134090.	12.7	6
84	ls polymeric substrate in influent an indirect impetus for the nitrification process in an activated sludge system?. Chemosphere, 2017, 177, 128-134.	8.2	4
85	The Application of Alginate Coated Iron Hydroxide for the Removal of Cu(II) and Phosphate. Applied Sciences (Switzerland), 2019, 9, 3835.	2.5	4
86	Stabilization of Zero-Valent Iron Nanoparticles for Enhanced In Situ Destruction of Chlorinated Solvents in Soils and Groundwater. , 2014, , 491-501.		3
87	Synergetic degradation of benzotriazole by ultraviolet and ultrasound irradiation. Desalination and Water Treatment, 2016, 57, 17955-17962.	1.0	3
88	The degradation pathway of aminosilicone polymer in aqueous microemulsion by Fenton process. Polymer Degradation and Stability, 2013, 98, 464-470.	5.8	2
89	Stabilization of Zero-Valent Iron Nanoparticles for Enhanced In Situ Destruction of Chlorinated Solvents in Soils and Groundwater. , 2009, , 281-291.		1